

Pathological and molecular evidence of LV adverse remodeling

- Histology
- Immunohistochemistry
- Electron microscopy
- RNA sequencing

Supplemental Figure 1. Experimental design employed to test the hypothesis that pediatric DCM patients do not undergo adverse remodeling. Transmural myocardial specimens were obtained from the apex and lateral wall of the left ventricle (LV) at the time of left ventricular assist device placement, cardiac transplantation, or donor heart procurement.

perivascular fibrosis

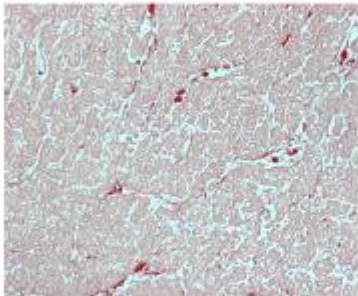
- grade 0: none
- grade 1: mild
- grade 2: moderate
- grade 3: severe

interstitial fibrosis

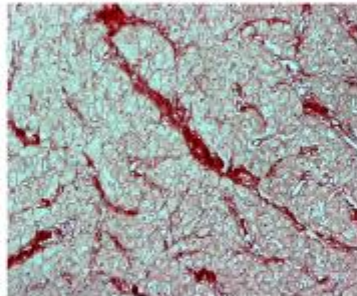
- grade 0: none
- grade 1: surrounding individual myocytes
- grade 2: replacement fibrosis
- grade 3: replacement fibrosis >50% of fields

perivascular fibrosis

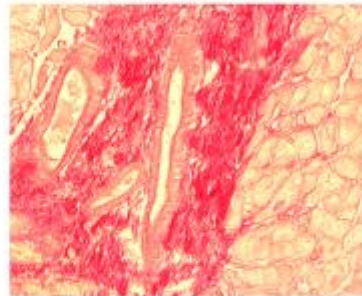
none (grade 0)



mild (grade 1)

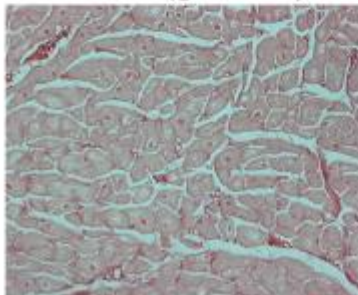


severe (grade 3)

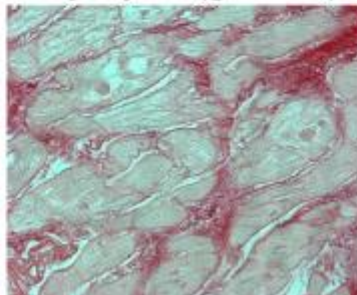


interstitial fibrosis

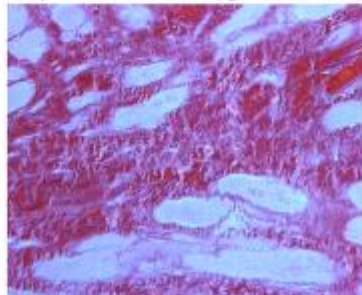
none (grade 0)



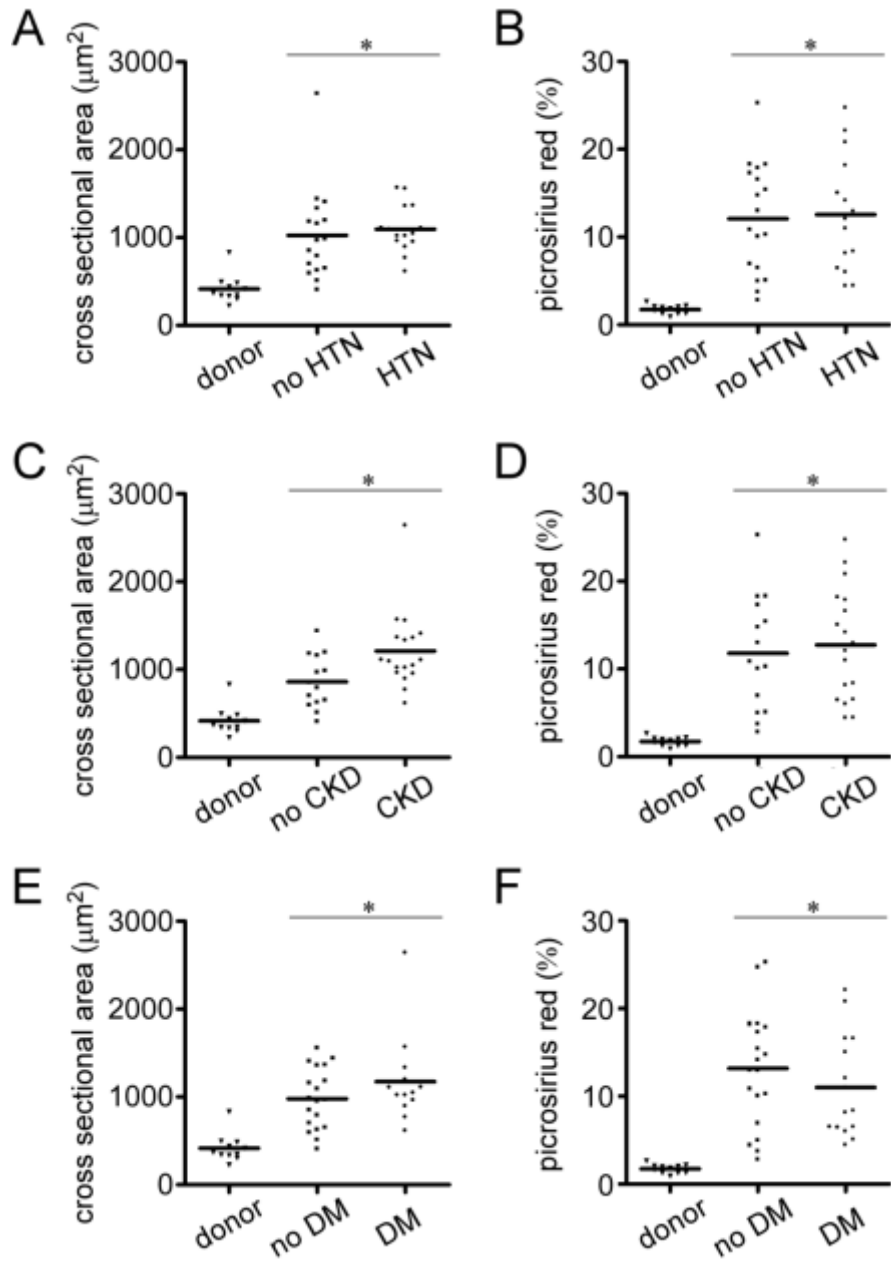
surrounding individual myocytes (grade 1)



replacement (grade 2/3)



Supplemental Figure 2. Fibrosis scoring system. Top, Descriptions of perivascular and interstitial fibrosis scores. Bottom, Examples of Picosirius red staining indicative of perivascular and interstitial fibrosis grades.



Supplemental Figure 3. Effect of cardiovascular comorbidities on pathological adverse remodeling in adult DCM. A-B, Measurements of cardiomyocyte hypertrophy (A) and myocardial fibrosis (B) stratified by the absence of hypertension (no HTN) or presence of hypertension (HTN). **C-D,** Measurements of cardiomyocyte hypertrophy (C) and myocardial fibrosis (D) stratified by the absence of chronic kidney disease (no CKD) or presence of chronic kidney disease (CKD). CKD was defined as stage 3 or greater chronic kidney disease. **E-F,** Measurements of cardiomyocyte hypertrophy (E) and myocardial fibrosis (F) stratified by the absence of diabetes (no DM) or presence of diabetes (DM). asterisks denotes $p<0.05$ compared to donor control. No significant differences were evident between adult DCM groups.

Supplemental Table 1. Pathways differentially upregulated in adult DCM.

GO:0055114: oxidation reduction	LDHA, PTGS2, KCNAB2, PTGS1, NDUFAB1, PRDX4, ADH1C, ADH1B, PRDX3, UQCRFS1, COX5A, AKR1C2, CH25H, HMOX1, GPX4, NDUFS8, SPR, CAT, NQO2, HPD, FTL, ACADM, CYP11A1, ACADS, NDUFC1, CDO1, POR, ACADVL, CYP4X1, ALDH1B1, CYBRD1, HSD11B1, STEAP2, ALDH9A1, SRXN1, MDH1, HSD17B10, PAM, TYRP1, CYP1B1, HSD3B7, RRM2B, FTH1, HADHA, GPD1L, FMO4, FMO3, ETFDH, DMGDH, GAPDH, ETFA, NDUFA4, GPD1, NOS1, FDXR, CYB561, MSRB2, SOD3, CYP4B1, SDHB, VAT1L, RDH10, DIO2, HSDL2, AKR1B1, CP, HPGD, RETSAT
GO:0009719: response to endogenous stimulus	ALPL, DHH, ATP6V0E1, CCL2, PTGS2, ALDOC, LEPR, PTGS1, ASNS, UQCRFS1, PRKAR2B, FOS, GSTM3, TNFRSF11B, GOT1, HMOX1, GPX4, IL1B, NKX2-5, MB, SPP1, TXNIP, BSG, AR, GNAO1, EGR2, CYP11A1, GATM, SOCS3, ACADS, IL1RN, GRIN2A, NR4A2, MGP, NR4A3, CDO1, CPS1, ADIPOQ, JUNB, GNAL, HMGCS2, PRKAR1B, GNG10, PEBP1, STEAP2, ASIP, MGST1
GO:0010033: response to organic substance	ATP6V0E1, AQP9, PTGS2, LEPR, PTGS1, PRDX3, UQCRFS1, PRKAR2B, FOS, TNFRSF11B, APOB, GSTM3, GOT1, CDKN2B, GSN, HMOX1, GPX4, IL1B, DDOST, CHRNA3, MB, PPP2R1A, BSG, AR, EGR2, CYP11A1, GATM, ACADS, SOCS3, GRIN2A, MGP, CDO1, JUNB, GNAL, CD83, THBD, HSPB1, PEBP1, CTSC, STEAP2, PTAFR, ALPL, DHH, CYP1B1, CCL2, PANX1, ALDOC, ACP5, ASNS, C1S, HSPA2, NKX2-5, SPP1, TXNIP, SELP, GNAO1, IL1RN, NR4A2, NR4A3, CPS1, ADIPOQ, EPHA3, HMGCS2, PRKAR1B, GNG10, MAFA, ASIP, SELE, MGST1, CD14
GO:0009611: response to wounding	FGF7, S100A8, F13A1, S100A9, TLR1, F2RL1, CXCR1, CXCR2, FOS, GSN, HMOX1, IL1B, CFD, GATM, LYZ, GRIN2A, CHST2, NFAM1, CDO1, TNFAIP6, THBD, PLA2G7, PEBP1, CTSB, PTAFR, CCL2, RTN4RL1, C6, CXCL2, NINJ1, CCL8, ABHD2, C1S, TMED7, IL17D, HRH1, SPP1, SELP, CR1, EFEMP2, IL1RN, CCL18, EPHA3, CCL13, LYVE1, CD59, BMPR1B, SELE, CD14, PLAU, BMP6
GO:0006954: inflammatory response	CCL2, S100A8, C6, CXCL2, S100A9, TLR1, CCL8, CXCR1, CXCR2, C1S, FOS, TMED7, IL17D, HRH1, HMOX1, IL1B, CFD, SPP1, SELP, CR1, IL1RN, CHST2, LYZ, NFAM1, CDO1, CCL18, EPHA3, TNFAIP6, CCL13, PLA2G7, BMPR1B, SELE, PTAFR, CD14, BMP6

GO:0006631: fatty acid metabolic process

ACAA2, TYRP1, ACADM, CPT2, PTGS2, ACADS, PTGS1, ACOT2, NDUFAB1, ECHS1, ACOT1, ADIPOQ, HADHA, HADHB, ACADVL, PRKAR2B, AKR1C2, PTGIS, PTGDS, PTGES, CH25H, ETFDH, ABCD2, LIPC, HPGD

Supplemental Table 2. Pathways differentially upregulated in pediatric DCM

GO:0006811: ion transport

KCNH1, SLC5A5, GRIK1, SLC9A4, TRPV1, SLC9A3, KCNJ10, AQP6, CNGB1, KCNJ14, KCNK10, KCNJ13, KCNQ5, SLC23A1, KCNQ3, MCOLN3, SLC24A3, SLC4A5, GRID1, KCNMA1, TRPM3, SLC12A8, PTGER3, TRPM8, SLCO4A1, SLC22A7, TRPA1, TRPM1, GABRR2, CATSPER2, CLIC6, KCNH6, PKDREJ, CLDN16, SLC38A4, ASZ1, RHBG, SLC38A11, SFXN2, KCNRG, PKD1L2, BEST3, COL9A1, SLC01A2, C1QTNF3, SLC30A8, HTR3B, HCN1, NOX5, SLC12A3, TRPC5, KCNB1, KCNV2, ATP2A1, SLC5A9, CHRNB2, SLC13A4, CACNA1D, CACNA1A

GO:0007155: cell adhesion

NPNT, PCDHGA9, NELL2, POSTN, PCDHGA6, PCDHGA4, NRCAM, CD96, WISP1, ROBO2, COL11A2, PCDHGA11, SDK1, LEF1, PCDHGB6, PTPRT, PCDHGB3, CD40LG, CPXM1, CNTN2, CLDN1, CLDN16, PPFA2, CLDN18, COL3A1, ASTN1, PCDHGC5, CDH1, PCDHGC4, CD72, COL9A1, LAMB4, COL17A1, COL6A6, COL27A1, FAT2, CD2, ACAN, FLRT3, NFASC, PCDH15, CLDN20, PCDH19, MUC4, LAMA1, DSG3, FREM2, NPHS1, DSC3, FBLN7, ITGAD, OMG, MUC5B, HABP2, MUC16

GO:0055085: transmembrane transport

KCNH1, SLC5A5, SLC9A4, TRPV1, SLC9A3, RHBG, CNGB1, SFXN2, AQP6, SLC47A2, KCNQ5, SLC23A1, KCNQ3, MCOLN3, SLC24A3, SLC30A8, HCN1, KCNMA1, TRPM3, SLC12A8, TRPM8, SLC22A9, SLC12A3, TRPC5, SLC22A7, KCNB1, TRPA1, RHD, ABCC13, KCNV2, ABCB5, TRPM1, CATSPER2, ATP2A1, KCNH6, SLC5A9, ABCC2, SLC13A4, SPNS1, CACNA1D, CACNA1A, ABCC6, SLC46A2

GO:0007601: visual perception

AIPL1, PCDH15, CNGB1, ABCA4, KCNV2, CRX, GABRR2, PROM1, CERKL, LRAT, PPEF2, CRB2, GRM6, PDC, CA4, CHRNB2, COL1A1, MERTK, ABCC6